Unmanned Aerial Vehicle Hub Detection Using Software-Defined Radio

1st Xuemei Huang
School of Information and Communication
Guilin University of Electronic Technology
Guilin, P. R. China
1436733855@qq.com

2nd Kun Yan
School of Information and Communication
Guilin University of Electronic Technology
Guilin, P. R. China
kyan5702@gmail.com

3rd Hsiao-Chun Wu
School of Electrical Engineering and Computer Scince
Louisiana State University
Baton Rouge, USA
wu@ece.lsu.edu

4th Yiyan Wu
Communications Research Centre
Ottawa, Canada
yiyan.wu@sympatico.ca

***Abstract*—The applications of unmanned aerial vehicles (UAVs) have increased dramatically in the past decade. Meanwhile, close-range UAV detection has been intriguing by many researchers for its great importance in privacy, security, and safety control. Positioning of the UAV controller (hub) is quite challenging but still difficult. In order to combat this emerging problem for public interest, we propose to utilize a software-defined radio (SDR) platform, namely HackRF One, to enable the UAV hub detection and localization. The SDR receiver can acquire the UAV source signals. The theoretical path-loss propagation model is adopted to predict the signal strength attenuation. Thus, the UAV hub location can be estimated using the modified multilateration approach by only three or more SDR receivers.**

***Index Terms*—Unmanned aerial vehicle (UAV), UAV hub, UAV hub detection and positioning, received signal strength indicator (RSSI), trilateration.**

I. Introduction

The use of *unmanned aerial vehicles* (UAVs), also known as *drones*, has become increasingly popular because of their low cost and easy deployment. Numerous civilian and commercial applications of drones have been emerging recently. Typical examples are agriculture [1], [2], traffic control [3], disaster monitoring [4], and border surveillance [5]. With more and more privately-owned drones being used, the number of incidents involving their misuse is also rising. From 2016 to 2017, unauthorized drones in the airports had caused serious threat to aircrafts' takeoff and landing [6]. Besides, malicious uses of drones have also been reported for carrying explosive, transporting drugs, stealing personal privacy, and attacking citizens. Therefore, it is very important to monitor and control the usage of drones, especially outdoors. Hence, in 2016, the US Federal Aviation Administration (FAA) signed an agreement to locate illegal drone operators.

Since then, researchers have proposed various solutions to positioning drones. In [7], an approach was proposed to localize unmanned aerial vehicles using multiple image sensors. Radar systems and acoustic sensors have also been used to locate drones [8]. However, localization of the drone control-signal source is a different and untackled problem. Neither image sensor nor radar system can be employed since the drone control-signal comes from an operator on the ground.

In our point of view, to analyze the radio signal sent from the controller and then localize the signal source is considered a potential solution to the drone controller positioning. The advantage of this new solution is its insensitivity to weather conditions, i.e., the detection can be undertaken even in dark, in fog, or in rain. Nevertheless, two challenges still have to be tackled before this new approach can take effect. First, it is hard to identify the associated drone with the particular drone controller of interest when multiple drones are in the scene. Second, it is difficult to separate and monitor individual drone control signals and address interference avoidance thereby. Third, how to localize a drone controller on the ground is still an open problem. Here we would like to focus on the drone-controller localization problem.

This paper presents a novel positioning method for spotting the drone control-signal source in a close range. The radio signal conveying drone control commands is acquired using the software defined radio (SDR) platform, namely HackRF One [9]. HackRF One is a *Universal Software Radio Peripheral* (USRP) capable of transmitting and receiving radio signals ranging from 1 MHz to 6 GHz. Most drones use spread-spectrum techniques in their remote-control systems, such as *direct sequence spread spectrum* (DSSS) and *frequency hopping spread spectrum* (FHSS), to mitigate interference from other communication systems including other drone-control signal(s). In this work, we concentrate on the FHSS drone-control signals since they are easier to analyze by our proposed scheme.

Once the drone-control signal data are acquired by the USRP, localization of such a controller takes place. In this work, the localization algorithm based on *trilateration* is investigated for its convenience and efficiency [10]. Trilateration is a range-based and decentralized localization algorithm based on simple geometry principles. Distance measures are the necessary information for trilateration. In practice, common distance estimation methods include *time of arrival* (TOA),

This work was supported by (NSFC 61163060, NSFC 61261034) from National Science Foundation of China, Research Enhancement Award from Guangxi Province (2011GXSFD01802) and (PF12067X, PF12091X) from Guangxi Key Laboratory of Communications and Signal Processing.

978-1-7281-2150-5/19/$31.00 ©2019 IEEE

time difference of arrival (TDOA), *enhanced observed time difference* (E-OTD), *round trip time* (RTT), and *received signal strength indicator* (RSSI) [11]–[16]. Since TOA, TDOA, E-OTD, and RTT require either the accurate time-stamps of the transmitted signal emission or the sophisticated set-up of the receiving antennae (in the fixed positions), we propose to use the RSSI distance measures for drone-controller localization here.

In this work, we propose a SDR based drone-controller localization approach. We first carry out field experiments to calibrate crucial parameters involved in the path-loss model, which can convert the RSSI measures to the accurate distances between the drone controller and multiple SDR receivers. Then the drone-controller can be located by the trilateration technique. According to real-world experiments, the localization accuracy can be within 2.47 meters on average.

The rest of this paper is organized as follows. The transmission model for this drone-controller localization problem is described in Section II. The details of the trilateration localization method are introduced in Section III. Real-world experiments to evaluate our proposed approach are presented in Section IV. Finally, conclusion will be drawn in Section V.

Nomenclature: $\mathbb{C}$, $\mathbb{Z}$, and $\mathbb{R}$ denote the sets of complex numbers, integers, and real numbers, respectively. $\otimes$ denotes linear convolution.

II. System Model

The positioning of a drone control-signal source requires multiple monitoring stations (receivers) outdoors to form a *monitoring and positioning network*. A *monitoring station* is simply a node that knows its coordinates. It is usually necessary to arrange at least three mobile or transportable monitoring stations with a certain distance in between each pair of stations. Figure 1 illustrates the geometric relationship among the monitor stations and the drone control-signal source to be localized. The drone control-signal is received by HackRF

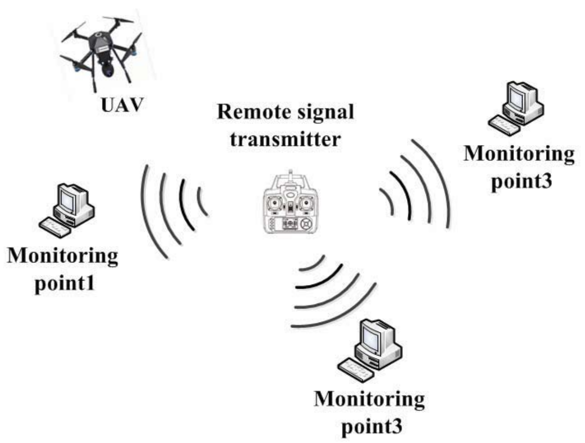

Fig. 1. The topological configuration of our proposed drone-controller localization scheme.

One and recorded by GNUradio (a software package [17]). The center frequency is tuned at 2.45 GHz, while the sampling frequency is 10 MHz. Figure 2 demonstrates the *spectrogram* of the recorded control-signal. This spectrogram manifests the frequency-hopping (FH) patterns of the drone control-signal. The received drone control-signal can be formulated by

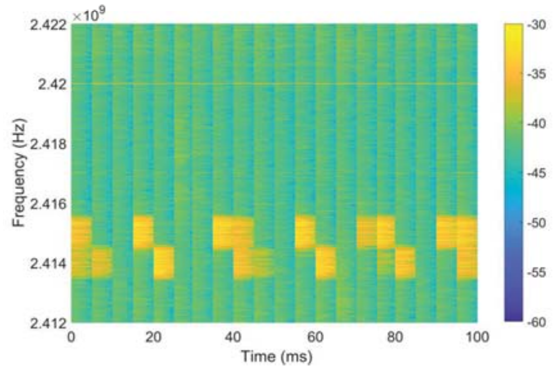

Fig. 2. Illustration of the spectrogram of the received drone-control signal acquired at (x_1, y_1).

$$r(t) = h(t) \otimes s(t) + n(t), \tag{1}$$

where $s(t)$ represents the transmitted FH signal and $h(t)$, $n(t)$ will be defined later on. The baseband modulation is *M*-FSK (*M*-ary frequency-shift keying) and then the FHSS scheme is employed. Thus, the transmitted FH signal $s(t)$ in Eq. (1) is given by

$$s(t) \overset{\text{def}}{=} \sqrt{2S}\,\cos\left[2\pi\left(f_i + \frac{m_l}{2T_s}\right)t + \theta_c\right],$$
$$(i-1)T_h + (l-1)T_s \geq t < (i-1)T_h + lT_s, \tag{2}$$

where S denotes the transmitting signal power, T_s is the baud duration, and T_h is the hop dwell time. Note that the hopping rate is $R_h \overset{\text{def}}{=} 1/T_h$. There are $N_s = T_h/T_s$ symbols within each hop. Furthermore, l denotes the data symbol index, i represents the hop index, and f_i, $i = 1, 2, \ldots, N$ represent the hopping frequencies. An FH carrier frequency f_i on the i^{th} hop is equally likely to be any among the equally-spaced frequencies which are statistically independent of each other from hop to hop. In this work, f_i are supposed to be the *a priori* knowledge. Besides, θ_c denotes the phase of the carrier signal, which is assumed to be uniformly distributed over $[0, 2\pi]$. The l^{th} data symbol on the i^{th} hop is m_l. The *M*-FSK information symbols are equally likely to be any integer over $\{1, 2, \cdots, H\}$ and are statistically independent of each other.

In addition, $n(t)$ in Eq. (1) represents the additive noise encountered in the propagation channel, which is assumed to be *additive white Gaussian noise* (AWGN), and $h(t)$ is the impulse response function of the wireless channel. The propagation models for UAV communications have been investigated in the literature [18]–[20]. Different propagation scenarios have been considered. Generally speaking, the RSSI is inversely proportional to the squared distance between the transmitter and the receiver in a free space. We follow this propagation (path-loss) model in this paper.

In practice, we utilize a wide-band SDR receiver with channelization using filter banks, which facilitate parallel processing of outputs from a series of narrow-band filters collectively covering the desired bandwidth. The structure of the signal-power estimator based on this channelization is illustrated in Figure 3. The fundamental filter-bank receiver consists of a bank of M filters spanning the total bandwidth. Channel outputs are collectively processed to estimate the RSSIs. The objective is to calculate the propagation distance from the remote controller to the HackRF One receiver. Since

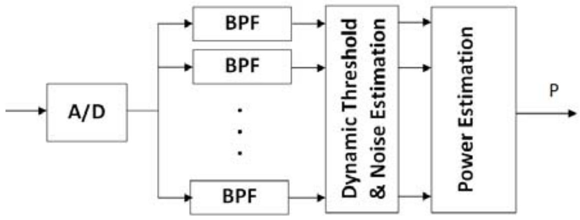

Fig. 3. The RSSI measurement system adopted in a monitoring station.

the bandwidth and hopping frequencies are assumed to be the *a priori* knowledge, M narrow-band filters, which have the impulse responses $l_i(t)$, $i = 1, 2, \ldots, M$, are designed to channelize the incoming FH signals. Thus, the i^{th} output of the filterbank is given by

$$u_i(t) = l_i(t) \otimes r(t). \tag{3}$$

Note that $l_i(t)$ is a narrow-band filter with center frequency f_i and bandwidth B. The RSSI P_i (in dB) of $u_i(t)$ can be estimated as

$$P_i \stackrel{\text{def}}{=} 10 \, \log_{10} \left[\frac{1}{W} \int_0^W \left| u_i(t) \right|^2 dt \right] - \beta, \tag{4}$$

where W is the integration time duration. We set $W = T_h$ and β denotes the *noise power* (in dB). How to estimate β will be presented in the following subsection.

The *average* received signal strength indicator (RSSI) P can be calculated by averaging the signal power over the M hopping frequencies. That is

$$P \stackrel{\text{def}}{=} \frac{1}{M} \sum_{i=1}^{M} P_i. \tag{5}$$

A. Noise-Power β Estimation

First, segment the output of the filter $l_i(t)$ in short-time windows (frames). If the signal-to-noise ratio is not too low, a simple energy-threshold can be used to detect the FH signal. As the noise is assumed to be stationary, the signal power can be assumed greater than or equal to the noise power. Hence, if the energy of a frame is significantly larger than the threshold, then the FH signal is present. Otherwise this frame contains noise only so that it will be used to update the current noise-power estimate. Let $X_i(\omega, k)$ be the power spectrum at frequency ω in the k^{th} frame of $u_i(t)$ given by Eq. (3), and $N_i(\omega, k)$ be the noise power-spectrum at frequency ω in the k^{th} frame of $u_i(t)$. A simple recursive formula to estimate the noise power $N_i(\omega, k)$ is thus given by

$$N_i(\omega, k) = \begin{cases} N_i(\omega, k-1), & \text{if} \quad \xi_i(\omega, k) > \upsilon, \\ (1-\gamma) N_i(\omega, k-1) + \gamma X_i(\omega, k), & \text{otherwise}, \end{cases} \tag{6}$$

where

$$\xi_i(\omega, k) \stackrel{\text{def}}{=} \frac{\sum_\omega X_i(\omega, k)}{\sum_\omega \xi_i(\omega, k-1)}. \tag{7}$$

Initialize $N_i(\omega, 0) = X_i(\omega, 0)$. It is under the assumption that the first frame of an received signal does not contain any FH signal. This restriction can be easily satisfied since one can search a series of frames to find the one with the minimum frame-energy for starting the noise-power estimation. Eq. (6) involves two parameters υ and γ which depend on the FH signal, where υ is related to the signal-to-noise ratio and γ characterizes the update speed of the noise-power estimation. Then the noise power of $u_i(t)$ in the k^{th} frame can be estimated as

$$\beta_i(k) \stackrel{\text{def}}{=} \sum_\omega N_i(\omega, k) d\omega. \tag{8}$$

Consequently, the *average* estimated noise-power β over K frames and M hopping frequencies can be estimated as

$$\beta \stackrel{\text{def}}{=} \frac{1}{MK} \sum_{k=0}^{K-1} \sum_{i=1}^{M} \beta_i(k). \tag{9}$$

III. Trilateration Localization Algorithm

According to [21], the *path-loss model* for signals propagating from a remote controller to a UAV is given by

$$P = -10 \, \zeta \, \log_{10}(d) + \alpha, \tag{10}$$

where ζ manifests the *signal propagation constant*, d denotes the distance between the transmitter and the receiver, and α is the received signal strength for propagation over a meter. Thus, according to Eq. (10), given P (from a measurement at the receiver), the *estimated communication-link distance* $\hat{d}$ can be calculated as

$$\hat{d} \stackrel{\text{def}}{=} 10^{\frac{\alpha - P}{10\,\zeta}}. \tag{11}$$

Figure 1 illustrates the topological set-up involving a drone control-signal source and three monitoring stations, where (x_q, y_q) denotes the coordinates corresponding to the q^{th} monitoring station, $q = 1, 2, 3$, (x_u, y_u) specifies the coordinates of the target object (UAV controller or signal transmitter), and d_q denotes the actual distance between the q^{th} monitoring station and the controller. Acquire individual received signals from the three monitoring stations and calculate the average

RSSI according to Eq. (5). Then, (x_u, y_u) can be estimated by solving the following system of equations:

$$\begin{cases} \sqrt{(|x_1 - \hat{x}_u|)^2 + (|y_1 - \hat{y}_u|)^2} = 10^{\frac{\alpha - P_1}{10\varsigma}}, \\ \sqrt{(|x_2 - \hat{x}_u|)^2 + (|y_2 - \hat{y}_u|)^2} = 10^{\frac{\alpha - P_2}{10\varsigma}}, \\ \sqrt{(|x_3 - \hat{x}_u|)^2 + (|y_3 - \hat{y}_u|)^2} = 10^{\frac{\alpha - P_3}{10\varsigma}}, \end{cases} \tag{12}$$

where P_q represents the received signal power measured by the q^{th} monitoring station and $(\hat{x}_u, \hat{y}_u)$ denotes the estimate of (x_u, y_u). Rewrite Eq. (12) and obtain

$$\mathcal{A}\, I = C, \tag{13}$$

where

$$\begin{aligned} \mathcal{A} &\stackrel{\text{def}}{=} \begin{bmatrix} 1 & -2x_1 & -2y_1 \\ 1 & -2x_2 & -2y_2 \\ 1 & -2x_3 & -2y_3 \end{bmatrix}, \\ I &\stackrel{\text{def}}{=} \begin{bmatrix} \hat{x}_u^2 + \hat{y}_u^2 \\ \hat{x}_u \\ \hat{y}_u \end{bmatrix}, \\ C &\stackrel{\text{def}}{=} \begin{bmatrix} 10^{\frac{2\alpha - 2P_1}{10\,\varsigma}} - x_1^2 - y_1^2 \\ 10^{\frac{2\alpha - 2P_2}{10\,\varsigma}} - x_2^2 - y_2^2 \\ 10^{\frac{2\alpha - 2P_3}{10\,\varsigma}} - x_3^2 - y_3^2 \end{bmatrix}. \end{aligned} \tag{14}$$

Consequently,

$$I = (\mathcal{A}^T \mathcal{A})^{-1} \mathcal{A}^T C, \tag{15}$$

and

$$\begin{aligned} \hat{x}_u &\stackrel{\text{def}}{=} I(2), \\ \hat{y}_u &\stackrel{\text{def}}{=} I(3). \end{aligned} \tag{16}$$

IV. Real-world Experiments

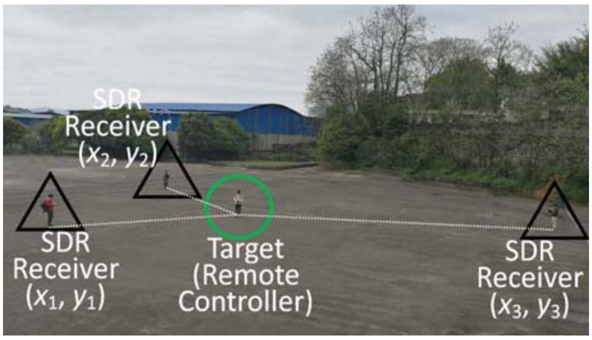

Fig. 4. Photo of the real-world field experiment.

The real-world experiment set-up is shown by Figure 4. The drone-controller, Wfly WFT07 transmitter (see [22]), is used as the control-source transmitter (shown by Figure 5). The SDR receiver, HackRF One with 2.4G antenna, is adopted as the receiver or the monitoring station (shown by Figure 6). The overall topological configuration of the experiment is illustrated by Figure 1.

MATLAB is invoked to perform the signal analysis. A filter-bank with a 20-tap length and a Hamming window is adopted to process the received radio-frequency (RF) signals. Then, short-time Fourier transform (STFT) is employed to obtain the spectrograms of the FH signals. Based on the experimental results, the RF signal transmitted from the controller has a total bandwidth of 2 MHz. The frequency-hopping mechanism is carried out across 10 channels and hopping occurs every 5 msec. A time-frequency illustration of two hopping frequencies is demonstrated by Figure 2. The effectiveness evaluation of our proposed new localization system is carried out by MATLAB. The received signal with a duration of 50 msec is collected to estimate the RSSI. The position of the UAV remote controller is determined based on the RSSIs measured by three monitoring stations.

Fig. 5. Photo of the UAV remote-controller (signal transmitter).

Fig. 6. Photo of the SDR receiver, HackRF One, for RF-signal acquisition.

The spectrogram of the received RF signal at (x_1, y_1) is exhibited by Figure 2. The frequency band from 2.412 to 2.422 GHz is illustrated in the figure. The time duration (window length) is 100 msec. An STFT is employed to generated Figure 2, where an FHSS signal is detected within the frequency band from 2.413 to 2.416 GHz. The RSSIs corresponding to the received FHSS signals through the propagation distances of 5 m, 10 m, . . ., 50 m are calculated according to Eq. (5). Figure 7 delineates the theoretical (according to Eq. (10)) and measured RSSIs over different propagation distances, where the red curve specifies the measured RSSIs and the blue curve specifies the theoretical RSSIs. Then, according to Eq. (11), the propagation distances d can be estimated from the acquired RSSIs. To evaluate the performance of our proposed localization scheme, the *propagation-distance estimation error-percentage* can be calculated by

$$d_e \stackrel{\text{def}}{=} \frac{\hat{d} - d}{d} \times 100\%, \tag{17}$$

where $\hat{d}$ is defined by Eq. (11). Figure 8 demonstrates the propagation-distance estimation error-percentages over different propagation distances.

In summary, the propagation-distance estimation error-percentage does not exceed 12% from experiments. Based on the location estimator given by Eqs. (15) and (16), the remote controller location is estimated and illustrated in Figure 9. Based on a segment of received signal within 250 msec, five estimated locations can be calculated. The averaged location-estimation error is 2.47 meters according to our experiments.

V. Conclusion

This paper introduces a novel technique for monitoring and locating the drone-controller on the ground. The UAV remote-control radio signal is captured and processed by the software-defined radio (SDR) platform, namely HackRF One. Then, the RSSI is measured to estimate the propagation distance between the transmitter (drone controller) and the receiver (SDR receiver). Finally, a trilateration localization technique is adopted to estimate the location of the drone controller. Experiments are carried out to validify the propagation model transforming the measured received signal strength into the propagation distance and it is very accurate in practice. Based on the received signal of a 250-msec duration, the average location-estimation error is within 2.47 meters, which is very promising for the future technological deployment to address public safety.

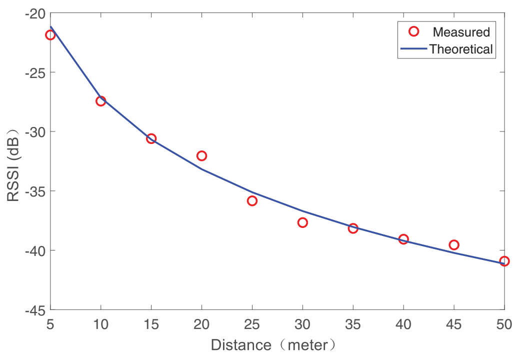

Fig. 7. The theoretical (according to the path-loss model) and measured (actual) RSSIs with respect to the propagation distance.

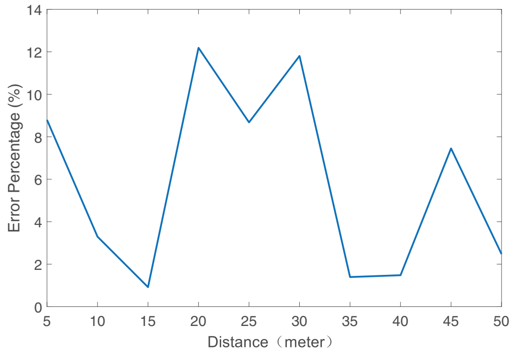

Fig. 8. Propagation-distance estimation error-percentage with respect to the propagation distance.

References

[1] P. Tripicchio, M. Satler, G. Dabisias, E. Ruffaldi, and C. A. Avizzano, "Towards smart farming and sustainable agriculture with drones," in *Proc. Int. Conf. Intelligent Environments (IE),*, July 2015, pp. 140–143.

[2] H. Xiang and L. Tian, "Development of a low-cost agricultural remote sensing system based on an autonomous unmanned aerial vehicle (UAV)," *Biosystems Engineering*, vol. 108, no. 2, pp. 174–190, Feb. 2011.

[3] C. Barrado, R. Messeguer, J. Lopez, E. Pastor, E. Santamaria, and P. Royo, "Wildfire monitoring using a mixed air-ground mobile network," *IEEE Pervasive Computing*, vol. 9, no. 4, pp. 24–32, Oct.-Dec. 2010.

[4] E. Semsch, M. Jakob, D. Pavlicek, and M. Pechoucek, "Autonomous UAV surveillance in complex urban environments," in *Proceeding of 2009 IEEE/WIC/ACM International Joint Conference on Web Intelligence and Intelligent Agent Technology*, Sep. 2009, pp. 82–85.

[5] Z. Sun, P. Wang, M. C. Vuran, M. A. Al-Rodhaan, A. M. Al-Dhelaan, and I. F. Akyildiz, "Bordersense: Border patrol through advanced wireless sensor networks," *Ad Hoc Networks*, vol. 9, no. 3, pp. 468–477, May 2011.

[6] "Drone delays 55 flights in china," http://news.statetimes.in/drone-delays-55-flights-china/, accessed: 2019-04-27.

[7] S. Y. Nam and G. P. Joshi, "Unmanned aerial vehicle localization using distributed sensors," *International Journal of Distributed Sensor Networks*, vol. 13, no. 9, pp. 1–8, 2017.

[8] I. Guvenc, "Detection localization and tracking of unauthorized UAS and jammers," in *Proceeding of Avionics Systems Conference (DASC)*, 2017, pp. 17–21.

[9] H. Miyashiro, M. Medrano, J. Huarcaya, and J. Lezama, "Software defined radio for hands-on communication theory," Aug. 2017, pp. 1–4.

[10] A. Savvides, H. Park, and M. B. Srivastava, "The bits and flops of the N-hop multilateration primitive for node localization problems," in *Proceedings of European Signal Processing Conference (EUSIPCO)*, Sep. 2002, pp. 111–121.

[11] Z. Xu, D. He, J. Li, L. Jiang, and H. Wang, in *Proceeding of 2017 IEEE 2nd Advanced Information Technology, Electronic and Automation Control Conference (IAEAC).*

[12] G. Fuxiang and Z. Xiaoguo, "Hybrid GPS/TDOA location algorithm in non-line-of-sight environment," in *Proceedings of 2012 2nd International Conference on Computer Science and Network Technology*, Dec. 2012, pp. 2033–2036.

[13] W. juan Ren, D. hui Hu, and C. biao Ding, "An improved method to sort and pair TDOA based on the correlation between TDOAs," in *Proceedings of 2011 IEEE CIE International Conference on Radar*, Oct. 2011, pp. 1041–1044.

[14] P. Vieira, N. Varela, N. Fernandes, N. Guedes, L. Varela, and N. Ribeiro, "A SON enhanced algorithm for observed time differences based geolocation in real 3G networks," in *Proceeding of International Symposium on Wireless Personal Multimedia Communications (WPMC)*, June 2013, pp. 1–5.

[15] H. Xiong, J. Tang, H. Xu, W. Zhang, and Z. Du, "A robust single gps navigation and positioning algorithm based on strong tracking filtering," *IEEE Sensors Journal*, vol. 18, no. 1, pp. 290–298, Jan 2018.

[16] H. Xiong, M. Peng, S. Gong, and Z. Du, "A novel hybrid rss and toa positioning algorithm for multi-objective cooperative wireless sensor networks," *IEEE Sensors Journal*, vol. 18, no. 22, pp. 9343–9351, Nov 2018.

[17] K. Vachhani and R. A. Mallari, "Experimental study on wide band FM receiver using gnuradio and RTL-SDR," in *Proceeding of 2015 International Conference ICACCI*, August 2015, pp. 1810–1814.

[18] A. Al-Hourani and K. Gomez, "Modeling cellular–to–UAV path-loss for suburban environments," *IEEE Wireless Communication Letter*, vol. 7, no. 2, pp. 82–85, 2018.
[19] S. Hayat, E. Yanmaz, and R. Muzaffar, "Survey on unmanned aerial vehicle networks for civil applications: A communications viewpoint," *IEEE Communications Survey and Tutorial*, vol. 18, no. 4, pp. 2624–2661, 2016.
[20] H. T. Kung, C. K. Lin, T. H. Lin, S. J. Tarsa, and D. Vlah, "Measuring diversity on a low–altitude UAV in a ground–to–air wireless 802.11 mesh network," in *Proceeding of IEEE Globalcom 2010*, Dec. 2010, pp. 1799–1804.
[21] E. Yanmaz, R. Kuschnig, and C. Bettstetter, "Channel measurements over 802.11a-based UAV-to-ground links," in *Proceeding of 2011 IEEE GLOBECOM Workshops (GC Wkshps)*, Dec 2011, pp. 1280–1284.
[22] L. Shenzhen WFLY Technology Development Co. (2019) WFT07 summary. [Online]. Available: http://en.wflysz.com/goods/detail/62.htm

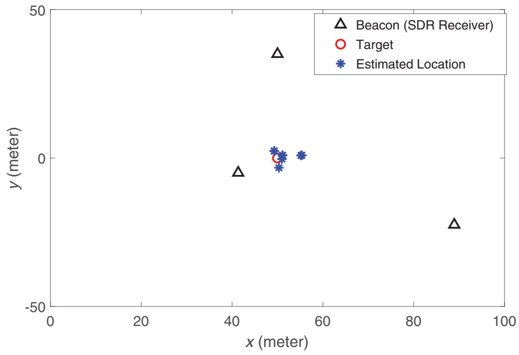

Fig. 9. Actual controller location (denoted by "◯"), locations of monitoring stations (denoted by "△"), and controller-location estimates (denoted by "⋆").